EurJIC
European Journal of Inorganic Chemistry

Full Papers
doi.org/10.1002/ejic.202100428

Chemistry Europe
European Chemical Societies Publishing

Ligand Effects in Carbon–Boron Coupling Processes Mediated by σ-BH Platinum Complexes

Pablo Ríos,[a] Francisco José Fernández-de-Córdova,[a] Javier Borge,[b] Natalia Curado,[a] Agustí Lledós,*[c] and Salvador Conejero*[a]

The reaction of tri-coordinated boranes (derived from dioxaborolanes and diazaborolanes) with cyclometalated low-electron count platinum complexes [Pt(NHC′)(NHC)][BAr^F] (NHC = I^{t}Bu^{i}Pr, IMes, IMes*) led, at low temperature, to the formation of the corresponding σ-BH species. Some of these species have been characterized by X-Ray diffraction methods showing a rare η^1-coordination mode. These compounds are thermally unstable and undergo a carbon-boron coupling process whose reversibility depends on the NHC ligand. DFT calculations indicate that the energy barriers required for C–B bond formation events (together with Pt–H bonds) are lower than the competitive reactions leading to C–H bond formation (and Pt–B bonds). However, the C–B coupling products appear to be formed under kinetic control with I^{t}Bu^{i}Pr ligands, whereas the relative low energy barrier leading to C–H bond formation is sufficiently low to form the thermodynamically more stable platinum boryl complexes at rt. The latter energy barrier is, nevertheless, too high for the systems bearing IMes and IMes* ligands.

Introduction

The interaction of tri-coordinated boranes, HBR_2, with transition metal complexes to form σ-BH species is a key step to induce the cleavage of the B–H bond on the way to form new B–X bonds (X=B, C, N).[1] σ-borane complexes are a rather well established family of compounds,[1k,2] although considerably more limited in number in comparison with the parent dihydrogen and σ-silane derivatives.[3] In most of the cases, the isolated σ-BH species are only involved in processes of cleavage of the B–H bond and/or exchange of the H atom with hydrides in metal compounds.[1k,2,4] However, this type of compounds can be engaged as intermediates in the formation of carbon-boron bonds, in particular in hydroboration processes,[1k,5] in the borylation of alkanes as described by Hartwig et al.[1j,6] or in other processes involving at some point the reaction of a borane and an alkyl complex.[7] In this sense, it is of particular relevance to understand the factors determining the formation of a carbon-boron bond when a metal-alkyl complex and a σ-BH borane are part of the same molecule. In this chemical situation, two possible scenarios can be foreseen: either the molecule evolves towards the formation of a metal-boryl (M–B) complex and an alkane (C–H) or to a metal-hydride (M–H) with concomitant formation of a carbon-boron bond (C–B) as exemplified in Scheme 1 for a σ-CAM (Complex Assisted Metathesis)[8] mechanism. The factors that direct the reaction towards one of those specific pathways are, therefore, particularly relevant when designing a catalytic process for the borylation of metal-alkyl bonds. Nevertheless, there is little information about these competitive reaction processes, due, in part, to the inherent difficulty in isolating (or detecting) σ-BH complexes bearing alkyl fragments in their structure.[1h,9] Very recently, we have been able to isolate and characterize some rare platinum examples of this kind (Scheme 2, complexes **2.1 a**–**c**).[10] Intriguingly, these compounds were unexpectedly

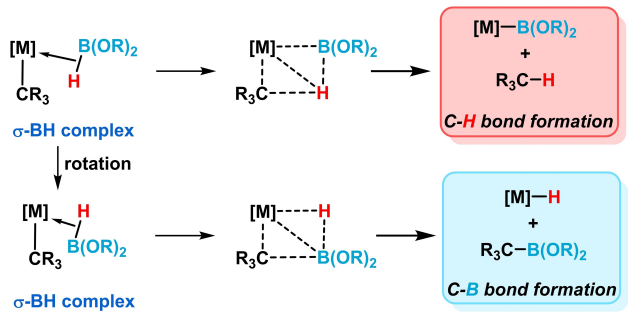

Scheme 1. Possible evolution pathways in the reaction of metal-alkyl complexes with boranes through a σ-CAM type mechanism.

[a] *Dr. P. Ríos, Dr. F. J. Fernández-de-Córdova, Dr. N. Curado, Dr. S. Conejero*
Instituto de Investigaciones Químicas (IIQ),
Departamento de Química Inorgánica, CSIC and
Universidad de Sevilla,
Centro de Innovación en Química Avanzada (ORFEO-CINQA),
C/Américo Vespucio 49, 41092 Sevilla, Spain
E-mail: sconejero@iiq.csic.es
[b] *Dr. J. Borge*
Departamento de Quimica Física y Analítica,
Centro de Innovación en Química Avanzada (ORFEO-CINQA),
Facultad de Química,
Universidad de Oviedo
C/Julián Clavería 8, 33006 Oviedo, Spain
[c] *Prof. A. Lledós*
Departament de Química,
Centro de Innovación en Química Avanzada (ORFEO-CINQA),
Universitat Autònoma de Barcelona
Edifici Cn, 08193 Cerdanyola del Vallés, Spain
E-mail: agusti@klingon.uab.es

Supporting information for this article is available on the WWW under https://doi.org/10.1002/ejic.202100428

Part of the "RSEQ-GEQO Prize Winners" Special Collection.

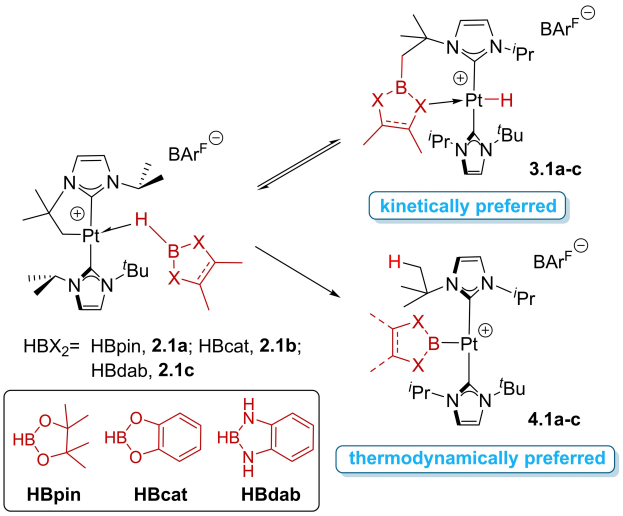

Scheme 2. Reversible C–B/C–H process observed for complexes **2.1 a–c**.[10]

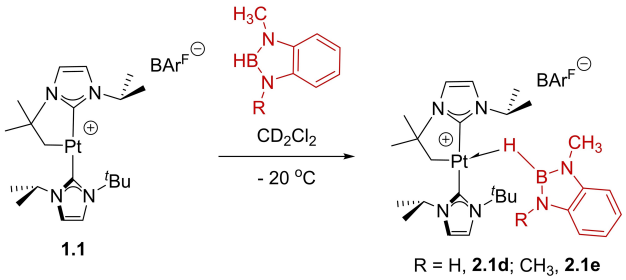

Scheme 3. Reaction of complex **1.1** with diamino boranes HBMedab and HBMe$_2$dab at low temperature.

involved in a reversible carbon-boron bond formation/cleavage process in which the formation of the carbon–boron bond (and a platinum hydride bond) was kinetically preferred whereas generation of a carbon–hydrogen bond (together with a platinum–boron bond) was thermodynamically favored, according to DFT calculations and low temperature NMR experiments. Thus, we set out to explore how the nature of the borane and NHC substituents influence the C–H/C–B bond forming reactions.

In this article we describe the reactivity of boranes with different sterereo-electronic properties (HBpin, HBcat, and substituted benzodiazaborolanes, with benzodiazaborolanes being more sterically demanding and having a less acidic boron atom and HBcat being the less sterically hindered and more acidic) with low-electron count cyclometalated Pt(II) complexes bearing bulky N-heterocyclic carbene ligands IMes, IMes* or less sterically congested I^{t}Bu^{i}Pr ligands.

Results and Discussion

Reactions of complex 1.1 with diaminoboranes

In our previous contribution we explored the reactivity of complex [Pt(I^{t}Bu^{i}Pr′)(I^{t}Bu^{i}Pr)[BAr^F] (**1.1**)[11] toward HBpin (pinacolborane), HBcat (catecholborane) and HBdab (1,3,2-benzodiazaborolane).[10] The reaction proceeded with the initial formation of the corresponding σ-BH complexes that are stable at temperatures ranging from −15 to +10 °C, being the diamino borane HBdab derivative (**2.1 c**) the most stable (Scheme 2). Similarly, the reaction of HBMedab (1-methyl-1,3,2-benzodiazaborolane) or HBMe$_2$dab (1,3-dimethyl-1,3,2-benzodiazaborolane) with complex [Pt(I^{t}Bu^{i}Pr′)(I^{t}Bu^{i}Pr)[BAr^F] at low temperature leads to the initial formation of the corresponding σ-BH complexes **2.1 d, e** (Scheme 3). These compounds have been characterized spectroscopically by low temperature NMR. The most significant feature

in the ^{1}H NMR is a broad signal of the bridging hydride (Pt–H–B) that resonates at −2.30 (**2.1 d**) and −2.11 ppm (**2.1 e**) with coupling constants to ^{195}Pt of 328.3 (**2.1 d**) and 320.0 Hz (**2.1 e**), comparable to those observed for complexes **2.1 a–c**, and clearly distinct to those observed for derivatives **3.1 a–c** (ca. 2200–2500 Hz).[10] These signals sharpen upon ^{11}B decoupling (See ESI Figure S12 and Figure S17). The ^{11}B{^{1}H} NMR spectra for **2.1 d, e** show a very broad signal at 19.5 and 20.3 ppm, respectively. Interestingly, some of the ^{1}H NMR signals for complex **2.1 d** appear rather broad at −20 °C, particularly that of the N–CH$_3$ group. Lowering the temperature to −40 °C indicated the presence of two species in a 3:1 ratio with similar chemical shifts for most of the protons, but clearly distinguishable by the bridging hydride, that shows two broad resonances at −2.00 and −2.40 ppm with $^1J_{Pt,H}$ of *ca.* 290 and 305 Hz, respectively. In addition, two different signals are observable for the NH, NCH$_3$ and the methinic protons of the *iso*-propyl fragments of the NHC in the same 3:1 ratio (see Figure S13 in the SI). All these signals merge into a single set of resonances (for each fragment) at about −20 °C. Further lowering of the temperature to −60 °C does not change significantly the ratio of the two species. According to theoretical calculations these two species are rotamers adopting different orientations of the HBMedab ligand, with similar energies (Figure S64). Complexes **2.1 d** and **2.1 e** are rather thermally stable and could be characterized by X-Ray diffraction studies of crystals grown at −20 °C. The X-ray representation of these two compounds is shown in Figure 1.

The structural parameters of complexes **2.1 d, e** show some deviations from those of the parent complex **2.1 c**. The angles defined by the C–Pt–H atoms are 171.1(9)° and 162.6(8)°, whereas those of the Pt–H–B fragment are 98(2)° (**2.1 d**) and 107(1)° (**2.1 e**). The Pt···B distances are 2.243(2) Å (**2.1 d**) and 2.272(3) Å (**2.1 e**), above of the sum of covalent radii for Pt and B (2.2 Å) and longer than those observed for Pt-boryl complexes.[10,12] The B–H bond distances of 1.22(3) Å (**2.1 d**) and 1.21(3) Å (**2.1 e**) are only marginally different to that in complex **2.1 c** (1.19(3) Å) and are slightly elongated with respect to those in free boranes.[13] These structural parameters indicate that the replacement of the NH groups by NCH$_3$ fragments has not an important steric effect in the interaction of the borane with the

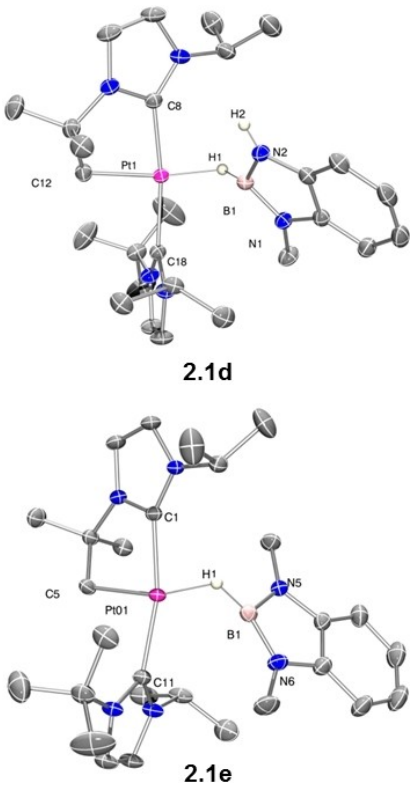

Figure 1. ORTEP-type representation of complexes **2.1 d** and **2.1 e** (ellipsoids at 30 % probability). All hydrogen atoms except that for the hydride ligand have been omitted for clarity.

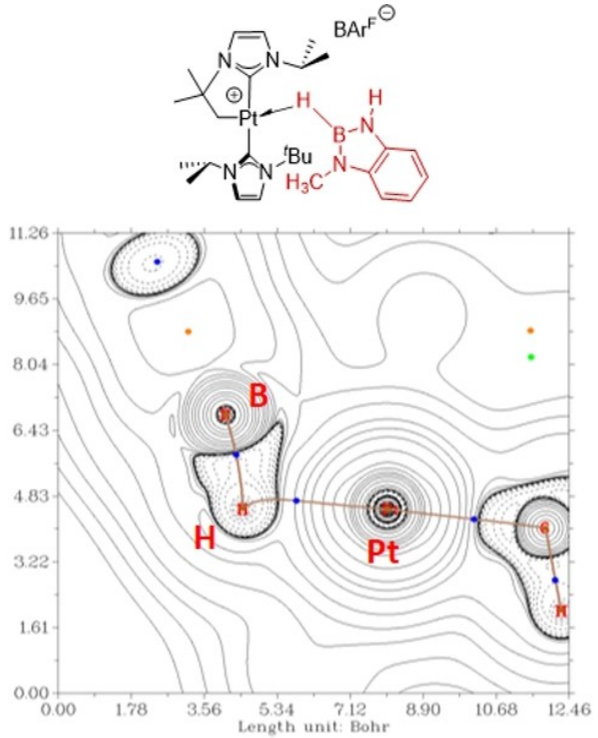

Figure 2. Plot of the Laplacian of the electronic density ($\nabla^2\rho$) of one of the rotamers of complex **2.1 d**.

Pt center and that, likely, the energies for bending the Pt–H–B angle leading to either an η^1 or η^2 type interaction are very low, as previously described.[10] In order to have a better picture of the bonding situation for complexes **2.1 d**,**e** a topological analysis of the electron density and its laplacian was carried out (see Figures S65–S67 and Figure 2). No bond critical point (BCP) between Pt and B was observed in any of the complexes, which suggests a very weak interaction between these two atoms (if any) and a η^1 coordination mode.[14] It is worth mentioning that in **2.1 d** two different orientations of the diamino borane were considered, based on the unsymmetrical character of the molecule and in line with the aforementioned low-temperature NMR experiments.

Complexes **2.1 d**,**e** are stable at temperatures below 15–20 °C. At higher temperatures a rearrangement takes place leading to the platinum hydride derivatives [Pt(H)(I^{t}Bu^{i}Pr-BX$_2$)(I^{t}Bu^{i}Pr)][BAr^F] (BX$_2$ = BMedab, **3.1 d**; BMe$_2$dab, **3.1 e**) after a carbon-boron bond coupling event (Scheme 4). Unfortunately, at the same temperature these hydride species evolve to the platinum boryl complexes [Pt(BX$_2$)(I^{t}Bu^{i}Pr)$_2$][BAr^F] (**4.1 d**,**e**), hampering the full characterization of these intermediates. Nevertheless, the presence of a hydride signal at δ −21.58 ($^1J_{Pt,H}$ = 1883.2 Hz; **3.1 d**) and δ −22.76 ($^1J_{Pt,H}$ = 1983.9 Hz; **3.1 e**) as well as the observation of broad resonances at *ca.* 30 ppm in the ^{11}B NMR spectra are signatures in line with our previous results using HBpin, HBcat and HBdab.[10] These species evolve slowly

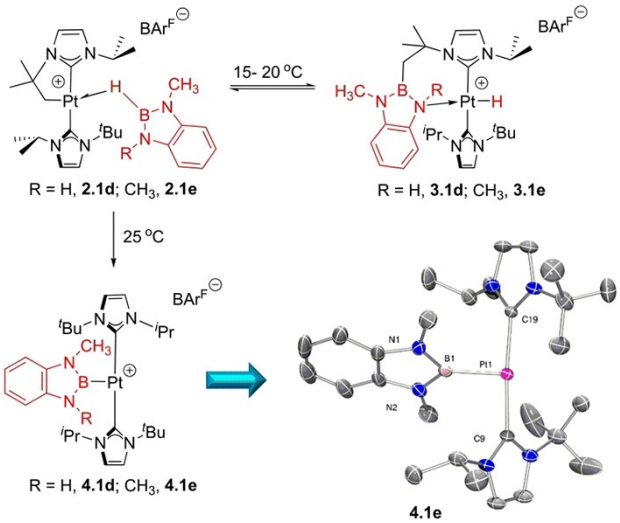

Scheme 4. Evolution of the σ-BH complexes **2.1 d**,**e** and ORTEP-type representation of the cationic fragment of complex **4.1 e** (hydrogen atoms have been omitted for clarity).

at room temperature over a period of 72 h leading to the platinum boryl species [Pt(BX$_2$)(I^{t}Bu^{i}Pr)$_2$][BAr^F] after a C–B bond cleavage reaction. The ^{1}H NMR spectra for these new compounds show a highly symmetric environment consistent with their formulation, whereas the ^{11}B NMR spectra show signals at 11.7 and 13.6 ppm for **4.1 d** and **4.1 e**,[15] respectively, exhibiting a large coupling to ^{195}Pt (~1400 Hz), as expected for a direct

interaction between the two atoms. Crystals suitable for X-ray diffraction studies were grown by slow diffusion of a concentrated solution of **4.1 e** into pentane (Scheme 4 bottom right shows the cationic fragment of this compound). The complex exhibits a characteristic T-shaped structure with a formally vacant site[16] in *trans* to the boryl ligand. The Pt–B bond distance of 2.000(4) Å lies at the lower end region for related systems.[10,12d,15b]

As inferred from previous theoretical calculations, the platinum boryl species are thermodynamically more stable than the platinum hydrides **3.1 d, e**, but formation of the latter is kinetically preferred. The reactivity observed with boranes HBMedab and $HBMe_2$dab does not differ significantly from that of HBdab, except that formation of the boryl complexes **4.1 d, e** requires longer reaction times (72 h *vs* 15 h for HBdab), likely due as a consequence of the steric constrains induced by the methyl groups on the borane fragments.

Reaction of complexes 1.2 and 1.3 with HBpin and HBcat

We then turned our attention to a platinum system bearing NHCs with different steric properties. To this aim we focused on complexes [Pt(IMes')(IMes)][BAr^F] (**1.2**) and [Pt(IMes*')(IMes*)][BAr^F] (**1.3**)[17] that have been also useful in the determination of the mechanism in the formation of carbon-silicon bonds by their reaction with silanes.[18] The reaction of these complexes with HBpin at rt led to a fast process (less than 15 min) that forms exclusively the platinum hydrides **3.2 a** and **3.3 a** arising from a carbon-boron bond coupling reaction (Scheme 5). Low temperature NMR experiments carried out at −60 °C of a mixture of complex **1.2** and HBpin allowed us to identify the σ-BH complex [Pt(HBpin)(IMes')(IMes)][BAr^F], **2.2 a** (Scheme 5). A rather complex ^{1}H NMR spectrum is observed for this complex at −60 °C (see ESI for details, Figure S46–48), but it clearly shows a broad resonance at −5.22 ppm with satellites arising from coupling to ^{195}Pt ($J_{H,Pt}$ = 355.0 Hz). These values are similar to those observed for complexes **2.1 a–e**. The ^{11}B{^{1}H} NMR spectrum for **2.2 a** only shows a broad signal for the excess of HBpin (ca 28 ppm) used in the experiment and the boron atom of the BAr^F anion (−6.7 ppm). Notably, the C–B coupling process leading to **3.3 a** starts to take place even at low temperatures (−25 °C).

The ^{1}H NMR of **3.2 a** and **3.2 b** reveals the highly unsymmetrical environment, but most particularly the presence of a broad resonance in the hydride region (−24.30, **3.2 a**; −25.10 ppm, **3.3 a**) exhibiting a coupling to ^{195}Pt of about 2200 Hz, together with a broad resonance in the ^{11}B NMR spectra at about 32 ppm are compatible with the proposed structure.[19] Complexes **3.2 a** and **3.3 a** are very sensitive towards trace amounts of adventitious water (present in the solvents used for purification) precluding their isolation in their pure form.[20] The water molecule binds the metal center leading to the corresponding 16-electron water adducts **3.2 a·H_2O** and **3.3 a·H_2O**. If pyridine is used as nucleophile, the corresponding adducts **3.2 a·py** and **3.3 a·py** can be isolated and fully characterized (see ESI for details). The structure of the

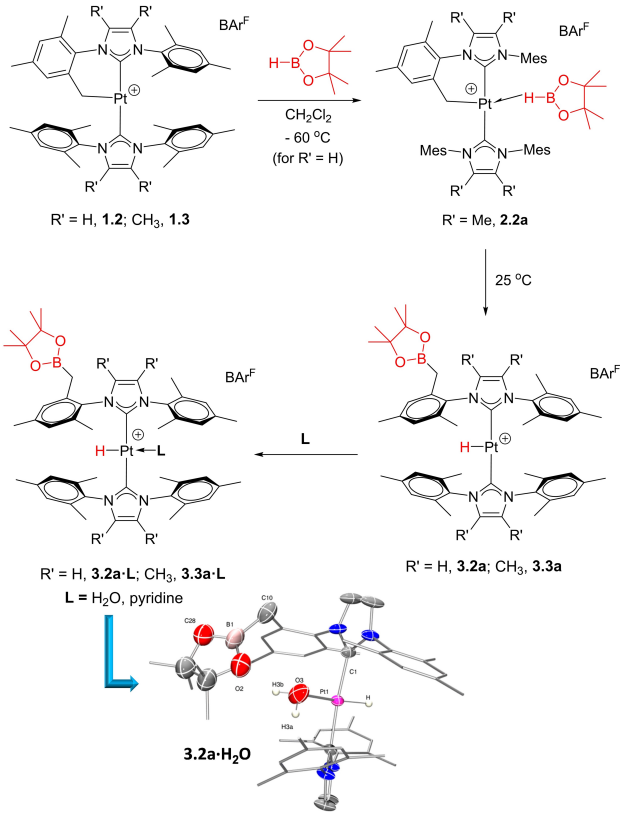

Scheme 5. Reactivity of complexes **1.2** and **1.3** toward HBpin and Lewis bases. Bottom: ORTEP-type view of the cationic fragment of complex **3.2 a·H_2O** (most of the carbon and hydrogen atoms of the molecule have been omitted for clarity).

water adduct **3.2 a·H_2O** was ascertained by X-ray diffraction studies (see Scheme 5, bottom). The molecule contains the two NHC ligands in the expected *trans* arrangement, one of them functionalized with the Bpin fragment with the new formed C–B bond. A hydride ligand and a water molecule complete the coordination sphere around the platinum center. One of the oxygen atoms of the Bpin moiety (O2), is oriented towards one of the hydrogen atoms of the water molecule and the close distances (d(O2···H3b) = 1.76 Å; d(O2···O3) = 2.63(1) Å) suggest hydrogen bonding character.

The reaction of **1.2** and **1.3** with HBcat was also performed. Again, a very fast reaction takes place that according to their ^{1}H and ^{11}B NMR spectra appear to give the C–B coupling products **3.2 b** and **3.3 b** (hydride signal *ca.* −25.0 ppm with $^1J_{Pt,H}$ ~2220 Hz and ^{11}B NMR at *ca.* 34 ppm). However, the reaction is not as clean as that with HBpin thwarting their full characterization and obtention in pure form. Although the crude reaction mixtures of these reactions do not show signs of formation of the products arising from C–H bond coupling (*i.e.* the boryl species [Pt(Bcat)$(IMes)_2$][BAr^F], **4.2 b**, and [Pt(Bcat)$(IMes^*)_2$][BAr^F], **4.3 b**, see below), apparently the hydride complexes **3.2 b** and **3.3 b** are able to further react with HBcat releasing hydrogen and giving rise to new species of unknown composition.

Very interestingly, compounds **3.2 a** and **3.3 a** are perfectly stable and remain unaltered after prolonged periods of time,

even under heating in methylene chloride (Scheme 6). These results clearly contrast with those observed when using complex **1.1**, for which the formation of the C–B bond is a reversible process that ultimately yields the platinum boryl species **4.1 a**–**e**. The first question that arises is if the platinum boryl complexes with IMes and IMes* are sufficiently stable to be isolable. In this sense we envisioned an alternative route to prepare them by reaction of the platinum hydrides [Pt(H)(IMes)$_2$][BAr^F] (**5.2**) and [Pt(H)(IMes*)$_2$][BAr^F] (**5.3**) with HBpin (Scheme 6). The reaction takes place smoothly under mild heating (60 °C), leading (quantitatively by NMR spectroscopy) to the boryl complexes [Pt(Bpin)(IMes)$_2$][BAr^F] (**4.2 a**) and [Pt(Bpin)(IMes*)$_2$][BAr^F] (**4.3 a**) in moderate isolated yields. The compounds are stable and can be stored in the absence of moisture indefinitely. The structure of **4.2 a** has been ascertained by X-ray diffraction studies (Figure 3). It shows structural metric parameters in line with complexes **4.1 c**,**e** (Pt–B bond length = 2.029(4)Å), with the two IMes ligands in a *trans* position and the Bpin fragment in *trans* to the formally vacant site (the closest H atom to platinum lies at 2.93 Å; note that these boryl compounds do not bind water in contrast to hydride derivatives **3.2 a** and **3.3 a**, possibly due to the higher trans influence of the boryl ligand in comparison to the hydride).[21] HBcat also reacts with platinum hydride complexes **5.2** and **5.3** generating the corresponding boryl complexes **4.2 b** and **4.3 b** (Scheme 6), but at variance with HBpin the reaction is very fast at 25 °C. The structure of **4.3 b** was confirmed by X-ray diffraction studies (Figure 3, right). This difference in reactivity might explain the difficulties in isolation of **3.2 b** and **3.3 b** (as mentioned above these hydrides also react with HBcat leading to mixtures of products).

Thus, the fact that the C–B coupling products **3.2 a** and **3.3 a** do not evolve to the boryl species **4.2 a** and **4.3 a** might be related to either a higher energy reaction pathway for a reversible C–B bond cleavage process (as in Scheme 1) or a different mechanistic route in which formation of the C–B bond

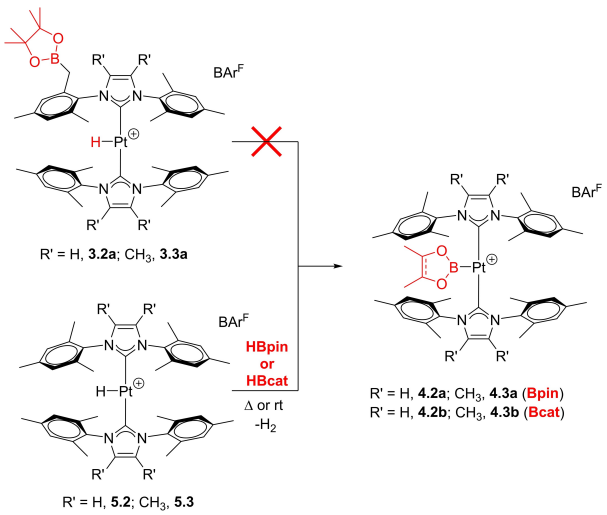

Scheme 6. Potential synthetic routes to obtain complexes **4.2 a**,**b** and **4.3 a**,**b**.

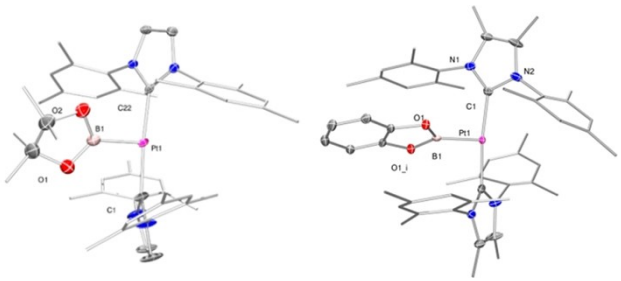

Figure 3. ORTEP-type view of the cationic fragment of complexes **4.2 a** (left) and **4.3 b** (right). Some carbon atoms and the hydrogen atoms of the molecule have been omitted for clarity.

is favored over the C–H one. To clarify this point we carried out DFT calculations (M06 functional) in dichloromethane solvent (SMD continuum model) on the different possible reaction pathways (see Supporting Information for details). Firstly, the reaction between cyclometalated complex **1.2** and HBpin was explored to compare the resulting energy surface to that previously observed when using complex **1.1**.[10] Thus, the influence of the NHC ligands on the C–B bond formation/cleavage can be evaluated on both systems. Therefore, C–H and C–B bond formation pathways (Scheme 1) were considered in complexes possessing both NHC ligands in *trans* and *cis* geometries (See Figures S68-S71 for every energy profile). We started analyzing the possible reaction pathways leading to complex **3.2 a**. A C–B bond formation pathway with a *trans* arrangement of the NHC ligands yielded too energy demanding transition states (> 30 kcal mol^{-1}) to be experimentally feasible. However, as previously found for the reaction of **1.1**,[10] considering a *cis* orientation of the IMes groups afforded an energy landscape that agrees well with the results summarized in Scheme 5 (Figure 4). The first step of this mechanism is the isomerization of cyclometalated complex **1.2** via transition state **TS1** (16.0 kcal mol^{-1}). The steric bulk of the IMes ligands makes this isomerization more difficult for **1.2** than for **1.1** (barriers of 16.0 and 12.8 kcal mol^{-1}, respectively), but reachable at the reaction conditions. The stabilities of the *cis*- isomers of **1.2** and **1.1** are, however, alike (relative Gibbs energies of 13.0 and 11.1 kcal mol^{-1}, respectively). This step yields species **1.2-*cis***, which is 13.0 kcal mol^{-1} above its *trans* isomer. The C_{NHC}–Pt–C_{NHC} angle in this compound is 119.2°, which is slightly wider than that observed for **1.1** (112.6°) as a consequence of the increased steric bulk of the NHC ligands. Coordination of HBpin is almost isoenergetic (**2.2 a-*cis***, 13.2 kcal mol^{-1}), after which the C–B and Pt–H bonds are forged in a concerted manner in **TS2**. This transition state is located 22.0 kcal mol^{-1} above the origin and yields species **Int1-*cis*** (15.5 kcal mol^{-1}), which still bears both NHC ligands in a *cis* geometry and it exhibits an agostic interaction through the methylene unit (Pt–H = 2.06 Å, C–H–Pt = 113°). However, the steric hindrance of the IMes groups is evident once again by observing the C_{NHC}–Pt–H angle of 169.5°, which is more acute than that observed for its I^{t}Bu^{i}Pr analogue (174.9°). Orienting the carbene ligands in a *trans* geometry gives **3.2 a**, the second most stable species of the

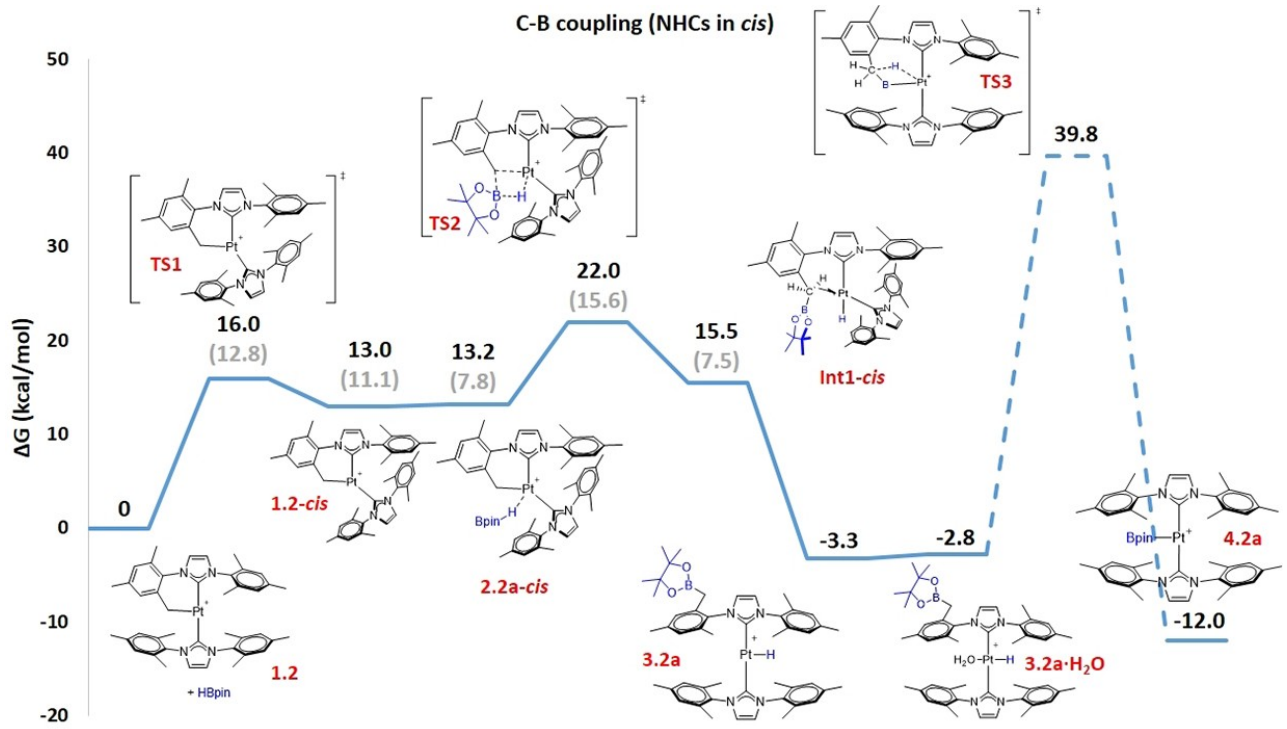

Figure 4. Gibbs energy profile in dichloromethane for the C–B coupling reaction between **1.2** and HBpin (NHC ligands in *cis*). Gibbs energies at 298 K in kcal mol^{-1}. The Gibbs energy of **1.2** + HBpin has been taken as zero-energy. Energy values in grey correspond to the analogous species using complex **1.1** instead of **1.2** (for comparison purposes).

energy profile (−3.3 kcal mol^{-1}). Coordination of adventitious water to the vacant position of this complex gives experimentally observed **3.2a·H_2O**, only 0.5 kcal mol^{-1} above.[22] Overall, the process needs to overcome energy barriers comparable to those observed for the I^{t}Bu^{i}Pr system[10] (I^{t}Bu^{i}Pr: 15.6 kcal mol^{-1} vs IMes: 22.0 kcal mol^{-1}). From here, cleaving the C–B bond to give boryl species **4.2a** would require overcoming **TS3**, but this barrier is too high in energy (39.8 kcal mol^{-1}) to be reached under the experimental conditions. This proposed mechanism fits well with **3.2a·H_2O** being the only observed species at the end of the reaction.

Then, we explored the energy costs for the competitive reaction pathway leading to a C–H bond coupling process. Expectedly, too high energy barriers (41.8 kcal mol^{-1}, Figure S71 in the ESI) have been calculated for a reaction pathway in which the IMes ligands are in a *trans* disposition. Importantly, C–H bond forming scenarios involving a *cis* rearrangement of the IMes ligands also gave very high energy barriers (> 35 kcal mol^{-1}, Figure 5), in agreement with the lack of experimental observation of **4.2a** by NMR. This value is considerably higher than that observed for the platinum system bearing the I^{t}Bu^{i}Pr ligand (complex **1.1**), for which a barrier of 22.1 kcal mol^{-1} was calculated.[10] This latter barrier can be, however, surpassed under the experimental reaction conditions (25 °C), which explains the reversibility of the process for the C–B bond formation/cleavage observed for complex **1.1**.

Next, the formation of boryl complexes **4.2a** and **4.2b** from hydride complex **5.2** was computed. Contrary to that observed for the previous energy profiles, mechanisms involving complexes in a *cis* geometry gave the highest barriers (Figures S74 and S75), making σ-CAM mechanisms unfeasible for this transformation. The potential energy surface for the reaction between **5.2** and HBcat is depicted in Figure 6. Since this mechanism only involves species in a *trans* geometry, it is much simpler; coordination of the borane is slightly exergonic, giving **6.2b** −1.9 kcal mol^{-1} below the energy reference. Upon binding (Pt–H–B = 113.0°), the B–H bond slightly weakens based on its elongation (1.219 Å in the σ complex vs. 1.178 Å in the free borane). Then, the H (from Bcat) fragment migrates in an orbiting fashion[23] assisted by the Pt atom toward the hydride ligand in **TS7** (26.3 kcal mol^{-1}). This transition state has a dihydride nature, pointing out a mechanism involving concerted B–H oxidative addition/H_2 reductive elimination for the formation of the boryl species. Interestingly, the Pt–H distance of the migrating hydride is shorter (1.520 Å) than that of the H atom *trans* to the Bcat fragment (1.681 Å) due to the *trans* influence of the latter. After the transition state, complex **4.2b·H_2** is formed (−2.8 kcal mol^{-1}), which features a dihydrogen molecule bound to the metal *trans* to the Bcat moiety. Release of H_2 from the complex affords boryl species **4.2b**, the most thermodynamically stable compound of the profile, in agreement with the experimental observations. Upon H_2 release, the Pt–B bond distance decreases from 1.988 to 1.968 Å. The reaction between complex **5.2** and HBpin leading to boryl complex **4.2a** follows the same reaction pathway,

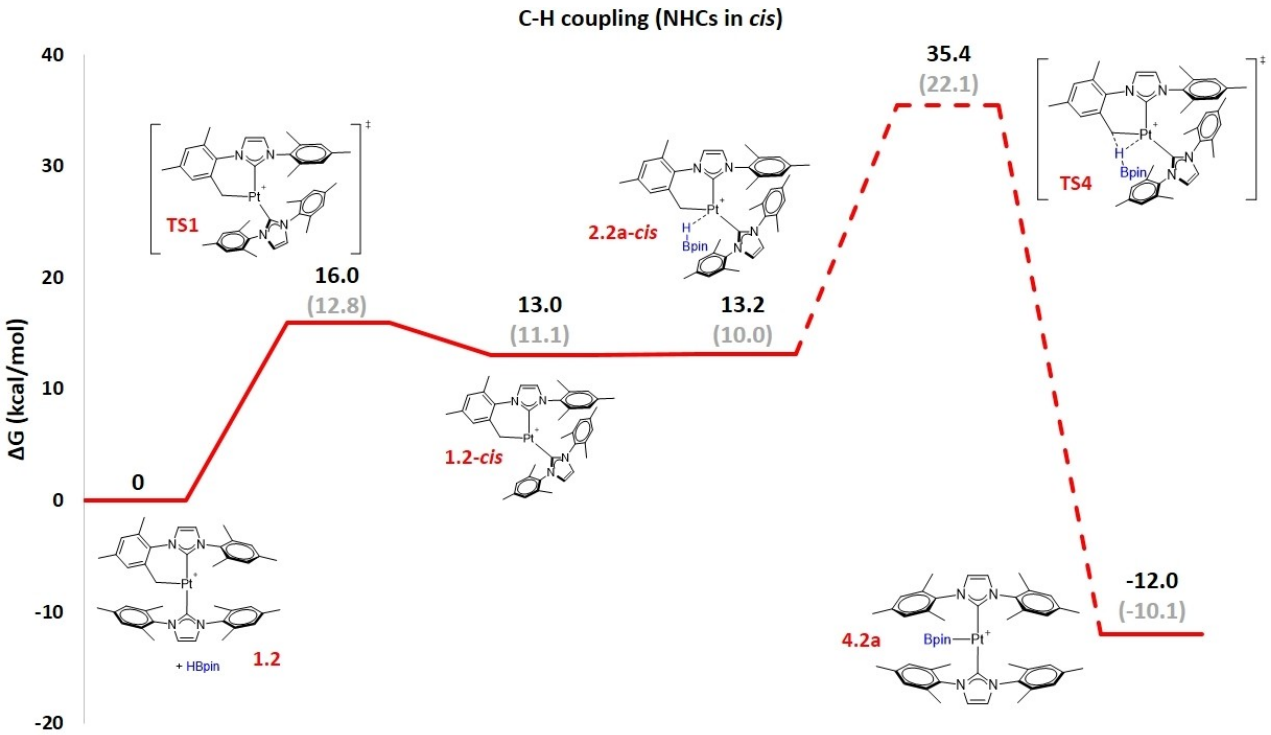

Figure 5. Gibbs energy profile in dichloromethane for the C–H coupling reaction between **1.2** and HBpin (NHC ligands in *cis*). Gibbs energies at 298 K in kcal mol^{-1}. The Gibbs energy of **1.2** + HBpin has been taken as zero-energy. Energy values in grey correspond to the analogous species using complex **1.1** instead of **1.2** (for comparison purposes).

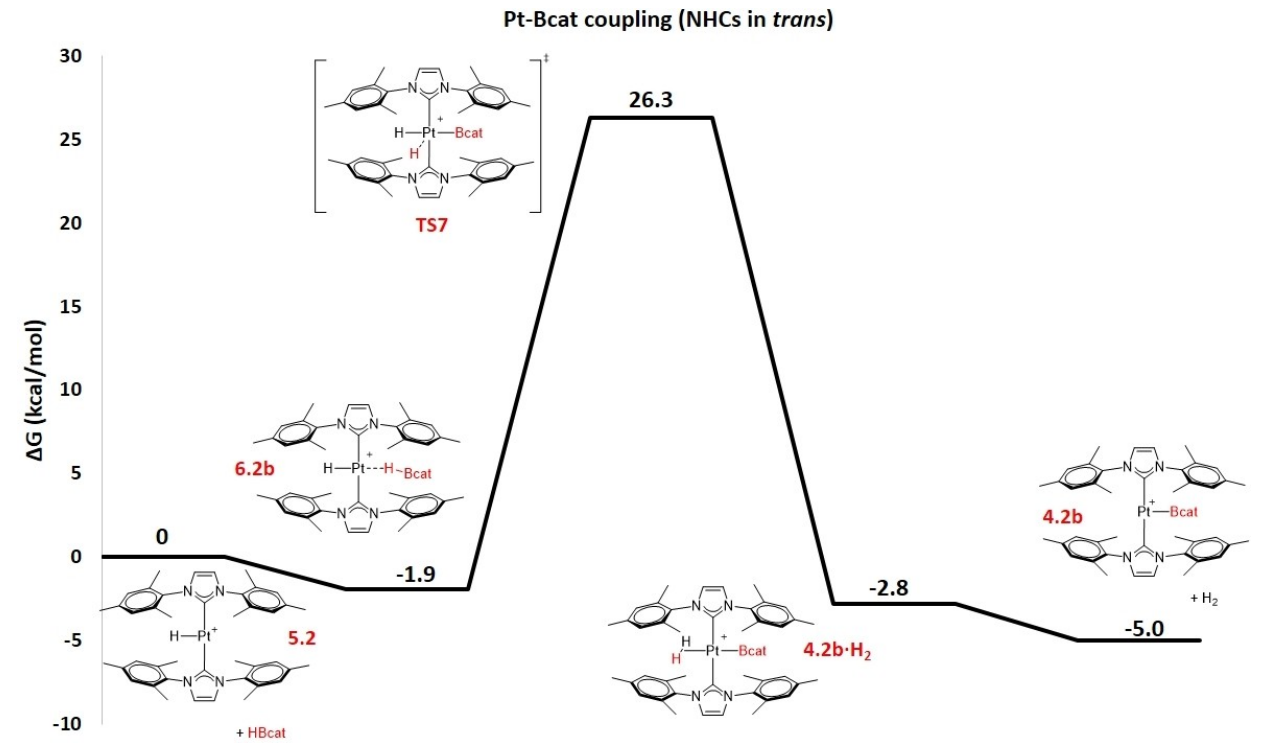

Figure 6. Gibbs energy profile in dichloromethane for the reaction between **5.2** and HBcat. Gibbs energies at 298 K in kcal mol^{-1}. The Gibbs energy of **5.2** + HBcat has been taken as zero-energy.

although with higher energetic barriers in agreement with experimental observations (see Figure S73 in the ESI).

On the other hand, the reaction of complexes **1.2** and **1.3** with diamino boranes HBdab and HBMedab led to complex mixtures of products from which no clear conclusions could be drawn. No reaction was observed between complex **1.2** and $HBMe_2dab$, even under heating at 60 °C. Nevertheless, $HBMe_2dab$ reacts slowly with complex **1.3** over a period of 40 h at rt but, interestingly, the major product observed when monitoring this reaction by NMR spectroscopy appeared to be platinum boryl complex **4.3e** (Scheme 7).[24] However, another species which seem to have a rather unsymmetrical environment is formed at the same time in small amounts precluding isolation of complex **4.3e** in its pure form. The ^1H NMR of complex **4.3e** reveals a highly symmetric environment in line with complexes **4.2a**,**b** and **4.3a**,**b**. The ^{11}B NMR spectrum shows, besides the signal for the BAr^F anion, a broad resonance at *ca.* 10 ppm for the BMe_2dab fragment in the expected region for this type of platinum boryl complexes.

The reasons underlying this reaction pathway are not entirely understood, but the increased steric hindrance of $HBMe_2dab$ in comparison with HBpin and HBcat (at the boron atom environment) might hamper the coupling of the carbon and boron atoms. With respect to the minor product, it is difficult to establish its nature based on NMR spectroscopy, and we speculate that it might be related to the competitive formation of the C–B coupling product. Unfortunately, we have not been able to ascertain its chemical nature. Investigations along these lines are currently undertaken and will be reported in due course.

Conclusion

The reaction of the 14-electron Pt(II) complexes of general formula $[Pt(NHC')(NHC)][BAr^F]$ with a series of tri-coordinated boranes at low temperature led to the initial formation of the corresponding σ-BH complexes $[Pt(HBR_2)(NHC')(NHC)][BAr^F]$ some of which are sufficiently stable to be characterized by X-ray diffraction studies or to be detected by NMR spectroscopy. These compounds exhibit an uncommon η^1-coordination mode. At certain range of temperatures these systems evolve through a process that involves the formation of carbon-boron bonds, in which the nature of the borane does not appear to have an important impact other than their thermal stability. Thus, for platinum systems bearing the NHC ligand I^{t}Bu/^{i}Pr the formation of the C–B bond is a reversible process that, according to our previous observations,[10] can lead back to the σ-BH complexes that, at higher temperatures, evolve towards a competitive, energetically accessible, process leading to a thermodynamically more stable platinum-boryl complex and formation of a C–H bond, regardless of the nature of the borane. However, it has been found that the nature of the NHC ligand has an important effect on the energetic barriers that direct the σ-BH complexes in one direction or the other. For the IMes-based platinum system, formation of the C–B bond is energetically more favorable, requiring only 22 kcal mol^{-1} in a process that involves *trans* to *cis* isomerization of the NHC ligands. It is worth noting that in spite of the more thermodynamically stable platinum boryl complexes (**4.2a**) compared to their platinum hydride isomers (arising from a C–B coupling process, **3.2a**) the energetic barrier needed to form them is too high (35.5 kcal mol^{-1} in the best case scenario), therefore explaining why these systems are not able to undergo a reversible C–B process. These results indicate that productive formation of C–B bonds can be controlled by modifying the nature of the NHC ligands.

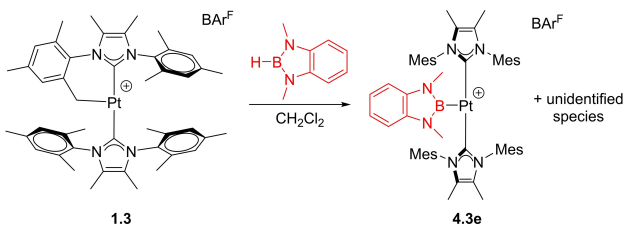

Scheme 7. Reaction of complex **1.3** with $HBMe_2dab$.

Experimental section

General: All manipulations were carried out using standard Schlenk and glovebox techniques, under an atmosphere of argon and of high purity nitrogen, respectively. All solvents were dried and degassed prior to use. *n*-Pentane was distilled over sodium and stored under Na/K alloy. Dichloromethane-d2 (CD_2Cl_2) was heated under reflux over calcium hydride, distilled under Argon and stored under 3 Å activated molecular sieves. NMR spectra were recorded on Bruker DRX-500, DRX-400 and DPX-300 spectrometers, and they were referenced to external $SiMe_4$ (δ 0 ppm) using the residual protio solvent peaks as internal standard (^1H NMR experiments) or the characteristic resonances of the solvent nuclei (^{13}C NMR experiments). ^{11}B NMR spectra were referenced to an external standard of $BF_3{\cdot}Et_2O$. Spectral assignments were made by routine one- and two-dimensional NMR experiments where appropriate. Elemental analysis was carried out with a LECO TruSpec CHN elementary analyser. $SMe_2{\cdot}BH_3$, HBpin and HBcat were purchased from Aldrich or TCI, stored under argon and used as received. Boranes HBdab, HBMedab and $HBMe_2dab$ were prepared from $SMe_2{\cdot}BH_3$ and 1,2-phenylenediamine, *N*-Methyl-1,2-phenylenediamine and *N*,*N*′-Dimethyl-1,2-diaminobenzene, respectively, as previously described.[25] Complexes $[Pt(I^tBu^iPr')(I^tBu^iPr)][BAr^F]$, **1.1**, $[Pt(IMes')(Mes)][BAr^F]$, **1.2**, and $[Pt(IMes*')(Mes*)][BAr^F]$, **1.3**, were obtained accordingly to published procedures.[11,17]

Synthesis of HMedab and $HBMe_2dab$: In a flame dried Schlenk tube *N*-Methyl-1,2-phenylenediamine (0.79 mL, 7.4 mmol) or *N*,*N*′-Dimethyl-1,2-diaminobenzene were dissolved, under argon in 20 mL of CH_2Cl_2. Then, $SMe_2{\cdot}BH_3$ (0.7 mL, 7.3 mmol) was added and the mixture was heated at 50 °C until no further H_2 evolution is observed (aprox. 2 h). The solvent was then removed under vacuum (at 0 °C in the case of $HBMe_2dab$) and the resulting solid (HBMedab) was washed with 10 mL of pentane whereas the oil arising from $HBMe_2dab$ was extracted with pentane (2×20 ml). HBMedab was obtained as an off-white solid in 89% yield, and $HBMe_2dab$ was obtained as a light brownish oil in 51% yield. **HBMedab**: ^1H-NMR (300 MHz, CD_2Cl_2, 25 °C): δ = 7.11–6.90 (m, 4H, CH), 6.74 (br, 1H, NH), 4.56 (br q, 1H, $J_{B,H}$ = 150 Hz, BH), 3.43 (s, 3H, NCH_3). $^{13}C\{^1H\}$ NMR (100 MHz, CD_2Cl_2, 25 °C): δ = 138.5 and 136.7 (C_q-N), 119.4, 119.2,

111.2 and 108.8 (CH). $^{11}B\{^1H\}$(128 MHz, CD_2Cl_2, 25 °C): δ = 25.0. **HBMe$_2$dab**: ^{1}H-NMR (300 MHz, CD_2Cl_2, 25 °C): δ = 7.05 (br, 4H, CH), 4.56 (br q, 1H, $J_{B,H}$ = 150 Hz, BH), 3.43 (s, 6H, NCH_3). $^3C\{^1H\}$ NMR (100 MHz, CD_2Cl_2, 25 °C): δ = 139.0 (C_q-N), 119.0 and 108.5 (CH), 31.0 (N–CH_3). $^{11}B\{^1H\}$(128 MHz, CD_2Cl_2, 25 °C): δ = 26.0.

Synthesis of complexes 2.1 d, e and 2.2 a. *General procedure*: Complex **1.1** (70 mg, 0.050 mmol) was dissolved in 0.4 mL of dry CD_2Cl_2 in a screw-cap NMR tube and cooled to −78 °C. Then, a borane (HBMedab, HBMe$_2$dab or HBpin) solution (0.060 mmol in 0.2 mL of CD_2Cl_2) was transferred via cannula into the NMR tube, and the mixture was shaken at −78 °C. The sample was analyzed by NMR in a pre-cooled (−30 °C) NMR apparatus. The ^{1}H NMR signals of complex **2.2 a** were too complex to be assigned. **Complex 2.1 d**: $^1H\{^{11}B\}$-NMR (400 MHz, CD_2Cl_2, −20 °C): δ = 7.75 (br, 8H, H_{ortho}-BAr^F), 7.57 (br, 4H, H_{para}-BAr^F), 7.26 and 7.13 (br s, 1H each, =CH), 7.10 (d, 1H, $J_{H,H}$ = 1.5 Hz, =CH), 7.06–6.91 (m, 5 H, =CH and CH-Bdan), 6.33 (br s, 1H, NH), 4.75 and 4.63 (br, 1H each, C*H*(CH_3)$_2$), 2.71 (br, 3H, N–CH_3), 2.36 (d + d, 1H, $J_{H,H}$ = 12.0 Hz, $J_{Pt,H}$ = 86.6 Hz, CH_2–Pt), 2.27 (d + d, 1H, $J_{H,H}$ = 12.0 Hz, $J_{Pt,H}$ = 71.0 Hz, CH_2–Pt), 1.81 (s, 9H, ^{t}Bu), 1.55 (br s, 3H, Pt–CH_2(C*H*$_3$)$_2$), 1.51 (d, 3H, $J_{H,H}$ = 6.5 Hz, CH(C*H*$_3$)$_2$), 1.41 (br, 6 H, Pt–CH_2(C*H*$_3$)$_2$ and CH(C*H*$_3$)$_2$), 1.25 (d, 3H, $J_{H,H}$ = 6.2 Hz, CH(C*H*$_3$)$_2$), 0.61 (br, 3H, CH(C*H*$_3$)$_2$), −2.30 (br s + d, 1H, $J_{Pt,H}$ = 328.3 Hz, Pt–H–B). $^{13}C\{^1H\}$ NMR (100 MHz, CD_2Cl_2, −20 °C): δ = 168.3 and 165.0 (Pt=C), 162.2 (q, $J_{C,B}$ = 50 Hz, C_{ipso}-BAr^F), 138.2 and 135.9 (C_q-Bdan), 134.8 (br, C_{ortho}-BAr^F), 128.8 (br q, $J_{C,F}$ = 30 Hz, C_{meta}-BAr^F), 124.5 (q, $J_{C,F}$ = 272 Hz, CF_3-BAr^F), 120.9 (=CH), 120.2 (2×CH-Bdab), 117.6 (br, C_{para}-BAr^F and =CH), 116.7 and 116.3 (=CH), 111.1 and 108.9 (CH-Bdan), 66.0 (Pt–CH_2*C*(CH_3)$_2$), 59.0 (C_q-^{t}Bu), 53.1 (*C*H(CH_3)$_2$), 33.7 (Pt–CH_2), 32.1 (CH_3), 31.3 (^{t}Bu), 29.7 (N–CH_3), 28.4 (CH_3), 24.9, 24.3, 21.7 and 21.2 (CH(*C*H$_3$)$_2$). $^{11}B\{^1H\}$(160 MHz, CD_2Cl_2, −20 °C): δ = 19.5 (broad, Bdan), −6.7 (s, BAr^F). **Complex 2.1 e**: $^1H\{^{11}B\}$-NMR (400 MHz, CD_2Cl_2, −30 °C): δ = 7.75 (br, 8H, H_{ortho}-BAr^F), 7.58 (br, 4H, H_{para}-BAr^F), 7.23, 7.12 and 7.10 (br s, 1H each, =CH), 7.04 (br, 5 H, =CH and CH-Bdan), 7.10 (br s, 1H, =CH), 4.62 (br, 1H, C*H*(CH_3)$_2$), 4.51 (sept, $J_{H,H}$ = 6.3 Hz, 1H, C*H*(CH_3)$_2$), 3.06 and 2.81 (s, 3H each, N–CH_3), 2.41 (d + d, 1H, $J_{H,H}$ = 11.2 Hz, $J_{Pt,H}$ = 88.0 Hz, CH_2–Pt), 2.23 (d + d, 1H, $J_{H,H}$ = 12.0 Hz, $J_{Pt,H}$ ~ 70 Hz, CH_2–Pt), 1.81 (s, 9H, ^{t}Bu), 1.57 (br s, 3H, Pt–CH_2(C*H*$_3$)$_2$), 1.51–137 (m, 9H, Pt–CH_2(C*H*$_3$)$_2$ and CH(C*H*$_3$)$_2$), 1.20 and 0.34 (br, 3H, CH(C*H*$_3$)$_2$), 1.25 (d, 3H, $J_{H,H}$ = 6.2 Hz, CH(C*H*$_3$)$_2$), 0.61 (br, 3H, CH(C*H*$_3$)$_2$), −2.11 (br s + d, 1H, $J_{Pt,H}$ = 320.0 Hz, Pt–H–B). $^{13}C\{^1H\}$ NMR (100 MHz, CD_2Cl_2, −30 °C): δ = 169.0 and 165.2 (Pt=C), 161.8 (q, $J_{C,B}$ = 50 Hz, C_{ipso}-BAr^F), 138.4 (C_q-Bdan), 134.8 (br, C_{ortho}-BAr^F), 128.8 (br q, $J_{C,F}$ = 30 Hz, C_{meta}-BAr^F), 124.5 (q, $J_{C,F}$ = 272 Hz, CF_3-BAr^F), 121.1 (=CH), 120.1 (CH-Bdab), 117.6 (br, C_{para}-BAr^F and =CH), 117.3, 116.8 and 116.5 (=CH), 108.4 (CH-Bdan), 65.9 (Pt–CH_2*C*(CH_3)$_2$), 59.2 (C_q-^{t}Bu), 53.9 and 53.1 (*C*H(CH_3)$_2$), 32.9 (CH_3), 32.6 (Pt–CH_2), 31.5 (^{t}Bu), 31.1 and 29.9 (N–CH_3), 28.4 (CH_3), 24.8, 24.2, 21.4 and 21.2 (CH_3 and CH(*C*H$_3$)$_2$). $^{11}B\{^1H\}$(160 MHz, CD_2Cl_2, −30 °C): δ = 20.3 (broad, Bdan), −6.7 (s, BAr^F). **Complex 2.2 a**: $^1H\{^{11}B\}$-NMR (400 MHz, CD_2Cl_2, −60 °C): δ = 7.75 (br, 8H, H_{ortho}-BAr^F), 7.55 (br, 4H, H_{para}-BAr^F), 7.43–6.71 (m, 12H, =CH), 2.721 (d + d, 1H, $J_{H,H}$ = 9.5 Hz, $J_{Pt,H}$ = 97.3 Hz, CH_2–Pt), 2.53 (d, 1H, $J_{H,H}$ = 9.5 Hz, $J_{Pt,H}$ not distinguible, CH_2–Pt), 2.46-1.68 (m, 33H, CH_3), 1.19 (s, 12H, CH_3-HBpin), −5.22 (br s + d, 1H, $J_{Pt,H}$ = 355.0 Hz, Pt–H–B). 166.7 and 166.4 (Pt=C), 162.2 (q, $J_{C,B}$ = 50 Hz, C_{ipso}-BAr^F), 139.1, 139.0, 136.7, 135.6, 135.5, 135.3, 134.9, 134.8, 134.1 and 133.8 (C_q, Mes and CH-Mes), 134.4 (br, C_{ortho}-BAr^F), 129.8-128.8. 124.2, 120.5 and 120.2 (m, CH-Mes, =CH), 129.2 (br q, $J_{C,F}$ = 30 Hz, C_{meta}-BAr^F), 125.1 (q, $J_{C,F}$ = 272 Hz, CF_3-BAr^F), 117.39 (br, C_{para}-BAr^F), 83.2 (C_q-Bpin), 24.4 (CH_3-Bpin), 22.7, 21.2, 20.9, 20.8, 19.2, 18.6, 18.3,18.2, 17.4 and 17.2 (CH_3-Mes), 14.4 (br, CH_2–Pt). $^{11}B\{^1H\}$(128 MHz, CD_2Cl_2, −60 °C): δ = −6.7 (s, BAr^F) (the signal for the coordinated HBpin was not observed).

Synthesis of complexes 4.1 d, e. *General procedure*: Complex **1.1** (80 mg, 0.057 mmol) was dissolved in 2 mL of dry CH_2Cl_2 and mixed via cannula with a solution of the corresponding borane (0.063 mmol) in 0.5 mL of CH_2Cl_2. The mixture was stirred at rt for 72 h and the solvent was removed under reduced pressure. Complexes **4.1 d** and **4.1 e** were washed with pentane (2×5 mL) and dried under vacuum. Compounds **4.1 d** and **4.1 e** can be crystallized by slow diffusion of a concentrated solution of CH_2Cl_2 into hexamethyldisiloxane (**4.1 d**) or pentane (**4.1 e**). (Yields: **4.1 d**: 60 %; **4.1 e**: 54 %). **Complex 4.1 d**: ^{1}H-NMR (400 MHz, CD_2Cl_2, 25 °C): δ = 7.73 (br, 8H, H_{ortho}-BAr^F), 7.57 (br, 4H, H_{para}-BAr^F), 7.23 (d, 2H, $J_{H,H}$ = 2.0 Hz, =CH), 6.97 (d, 2H, $J_{H,H}$ = 2.0 Hz, =CH), 6.91-6.78 (m, 4H, CH-Bdab), 5.78 (br s, 1H, NH), 5.01 (sept, 2H, $J_{H,H}$ = 6.7 Hz, C*H*(CH_3)$_2$), 2.96 (s, 3H, N–CH_3), 1.95 (s, 18H, ^{t}Bu), 1.08 (d, 12 H, $J_{H,H}$ = 6.7 Hz, CH(C*H*$_3$)$_2$). $^{13}C\{^1H\}$ NMR (100 MHz, CD_2Cl_2, 25 °C): δ = 179.3 (Pt=C), 162.2 (q, $J_{C,B}$ = 50 Hz, C_{ipso}-BAr^F), 138.4 and 136.3 (C_q-Bdan), 135.2 (br, C_{ortho}-BAr^F), 129.3 (br q, $J_{C,F}$ = 30 Hz, C_{meta}-BAr^F), 125.1 (q, $J_{C,F}$ = 272 Hz, CF_3-BAr^F), 120.5 (=CH), 119.24 and 119.18 (CH-Bdab), 117.9 (br, C_{para}-BAr^F), 116.1 (=CH), 110.1 and 108.2 (CH-Bdan), 59.1 (C_q-^{t}Bu), 55.2 (*C*H(CH_3)$_2$), 33.0 (^{t}Bu), 30.9 (N–CH_3), 22.8 (CH(*C*H$_3$)$_2$). $^{11}B\{^1H\}$(160 MHz, CD_2Cl_2, 25 °C): δ = 11.7 (s + d, broad, Bdan, $J_{Pt,B}$ ~ 1370 Hz), −6.6 (s, BAr^F). Elemental analysis calcd (%) for $C_{59}H_{56}B_2F_{24}N_6Pt$: C, 46.57; H, 3.71; N, 5.52; Found: C, 46.4; H, 3.7; N, 5.6. **Complex 4.1 e**: ^{1}H-NMR (400 MHz, CD_2Cl_2, 25 °C): δ = 7.74 (br, 8H, H_{ortho}-BAr^F), 7.57 (br, 4H, H_{para}-BAr^F), 7.23 (d, 2H, $J_{H,H}$ = 1.2 Hz, =CH), 6.99 (d, 2H, $J_{H,H}$ = 1.2 Hz, =CH), 6.93–6.85 (m, 4H, CH-Bdab), 4.85 (sept, 2H, $J_{H,H}$ = 6.3 Hz, C*H*(CH_3)$_2$), 2.95 (s, 6H, N–CH_3), 1.93 (s, 18H, ^{t}Bu), 1.01 (br, 12H, CH(C*H*$_3$)$_2$). $^{13}C\{^1H\}$ NMR (100 MHz, CD_2Cl_2, 25 °C): δ = 178.2 (Pt=C), 162.2 (q, $J_{C,B}$ = 50 Hz, C_{ipso}-BAr^F), 138.4 (C_q-Bdan), 135.2 (br, C_{ortho}-BAr^F), 129.3 (br q, $J_{C,F}$ = 30 Hz, C_{meta}-BAr^F), 125.1 (q, $J_{C,F}$ = 272 Hz, CF_3-BAr^F), 120.8 (=CH), 119.0 (CH-Bdab), 117.9 (br, C_{para}-BAr^F), 116.6 (=CH), 108.7 (CH-Bdan), 59.3 (C_q-^{t}Bu), 55.3 (*C*H(CH_3)$_2$), 33.2 (^{t}Bu), 30.8 (N–CH_3), 22.9 (br, CH(*C*H$_3$)$_2$). $^{11}B\{^1H\}$(160 MHz, CD_2Cl_2, 25 °C): δ = 13.6 (s + d, broad, Bdan, $J_{Pt,B}$ ~ 1420 Hz), −6.6 (s, BAr^F). Elemental analysis calcd (%) for $C_{60}H_{58}B_2F_{24}N_6Pt$: C, 46.92; H, 3.81; N, 5.47; Found: C, 47.1; H, 3.6; N, 5.4.

Synthesis of complexes 3.2 a, 3.3 a, 3.2 a·H2O, 3.3 a·H2O, 3.2 a·py and 3.3 a·py. *General procedure*: Complexes **1.2** or **1.3** (0.048 mmol) were dissolved in 0.7 mL of CD_2Cl_2 in a vial in the glovebox. The, HBpin (0.057 mmol, 8.3 μL) were added o this solution and transferred to an NMR tube. After 15 min at rt, complexes **3.2 a** and **3.3 a** were formed quantitatively according to ^{1}H NMR spectroscopy (see Figures S34–S36 and Figures S43–S45 in the ESI). The corresponding water and pyridine adducts were formed by addition of an excess of water (0.096 mmol, 1.7 μL) or pyridine (0.072 mmol, 5.8 μL). The reaction is instantaneous. The solvent was the removed under vacuum and the resulting solids washed with pentane (2× 5 mL). The solids were dried under vacuum leading to white or off-white solids. (Yields: **3.2 a·H_2O**: 65 %; **3.2 a·py**: 63 %; **3.3 a·H_2O**: 58 %; **3.3 a·py**: 53 %). **Complex 3.2 a·H_2O**: ^{1}H-NMR (400 MHz, CD_2Cl_2, 25 °C): δ = 7.73 (br, 8H, H_{ortho}-BAr^F), 7.56 (br, 4H, H_{para}-BAr^F), 6.98–6.90 (m, 10 H, CH-Mes + =CH), 6.84 and 6–78 (s, 1H, each =CH or CH-Mes), 6.91–6.80 (m, 13H, Mes, =CH), 2.45, 2.43, 2.41 and 2.38 (s, 1:2:1:1 ratio, 12H, CH_3-Mes), 2.10 (d, 1H, $J_{H,H}$ = 16.0 Hz, CH_2-Bpin), 1.90 (s, 6H, CH_3-Mes), 1.82 (s, 3H, CH_3-Mes), 1.77 (s, 6H, CH_3-Mes), 1.71 (s, 3H, CH_3-Mes), 1.72 (H_2O), 1.68 (br s, 4H, 1.82 (s, 3H, CH_3-Mes + CH_2-Bpin), 1.14 (s, 12H, CH_3-Bpin), −27.96 (s + d, 1H, $J_{Pt,H}$ = 1899.2 Hz, Pt–H). $^{13}C\{^1H\}$ NMR (100 MHz, CD_2Cl_2, 25 °C): δ = 176.9 and 176.5 (Pt=C), 162.2 (q, $J_{C,B}$ = 50 Hz, C_{ipso}-BAr^F), 139.7, 139.6, 139.4, 136.6, 136.5, 135.8, 135.7, 135.4, 135.0 and 134.9 (C_q, Mes), 136.2, 136.1, 135.9, 135.7, 135.59, 135.57, 135.5 (C_q-Mes and CH-Mes), 135.2 (br, C_{ortho}-BAr^F), 129.7, 129.5, 129.4 and 129.3 (CH-Mes), 129.2 (br q, $J_{C,F}$ = 30 Hz, C_{meta}-BAr^F), 128.3 (CH-Mes), 125.1 (q, $J_{C,F}$ = 272 Hz, CF_3-BAr^F), 122.9, 122.6 and 122.4 (1:2:1 ratio, =CH), 117.9 (br, C_{para}-BAr^F), 85.0 (C_q-Bpin), 24.7 and 24.5 (CH_3-Bpin), 21.34, 21.27, 21.24, 18.7, 18.0, 17.83. 17.75 and 17.6 (CH_3-Mes), 15.0 (br, CH_2-Bpin). $^{11}B\{^1H\}$(128 MHz, CD_2Cl_2, 25 °C): δ = 32.3 (br, Bpin), −6.6 (s, BAr^F). Elemental analysis calcd (%) for $C_{80}H_{74}B_2F_{24}N_5O_3Pt$: C, 53.02; H, 4.12;

N, 3.09; Found: C, 53.1; H, 4.3; N, 3.1. **Complex 3.2 a·py**: ^{1}H-NMR (400 MHz, CD_2Cl_2, 25 °C): δ = 7.75 (br, 8H, H_{ortho}-BAr^F), 7.55 (br, 4H, H_{para}-BAr^F), 7.52 (t, 1H, $J_{H,H}$ = 7.6 Hz, CH-py), 7.05 (d, 2H, $J_{H,H}$ = 7.6 Hz, CH-py), 6.97 (s, 4H, =CH), 6.91–6.80 (m, 13H, Mes, =CH and CH-py), 2.41 (s, 12H, CH_3-Mes), 1.70–1.58 (m, 24H, CH_3-Mes), 1.56 and 1.50 (d, 1H each, $J_{H,H}$ = 16.1 Hz, CH_2-Bpin), 1.14 and 1.11 (s, 6H each, CH_3-Bpin), −20.3 (s + d, 1H, $J_{Pt,H}$ = 1381.0 Hz, Pt–H). ^{13}C{^{1}H} NMR (100 MHz, CD_2Cl_2, 25 °C): δ = 173.8 and 173.9 (Pt=C), 162.2 (q, $J_{C,B}$ = 50 Hz, C_{ipso}-BAr^F), 151.3 (CH-py), 139.38, 139.36, 137.3 and 139.3 (C_q, Mes), 136.9 (CH-py), 136.2, 136.1, 135.9, 135.7, 135.59, 135.57, 135.5 (C_q-Mes), 135.2 (br, C_{ortho}-BAr^F), 129.43 and 129.37 (CH-Mes), 129.3 (br q, $J_{C,F}$ = 30 Hz, C_{meta}-BAr^F), 129.0 (CH-Mes), 128.9 (CH-py), 125.2 (CH-Mes), 125.1 (q, $J_{C,F}$ = 272 Hz, CF_3-BAr^F), 123.8, 122.6 and 122.0 (1:2:1 ratio, =CH), 117.9 (br, C_{para}-BAr^F), 84.1 (C_q-Bpin), 25.0 and 24.8 (CH_3-Bpin), 21.31, 21.26, 18.2 and 18.0 (CH_3-Mes), 17.1 (br, CH_2-Bpin). ^{11}B{^{1}H}(128 MHz, CD_2Cl_2, 25 °C): δ = 32.7 (very broad, Bpin), −6.6 (s, BAr^F). Elemental analysis calcd (%) for $C_{85}H_{77}B_2F_{24}N_5O_2Pt$: C, 54.50; H, 4.14; N, 3.74; Found: C, 54.8; H, 4.0; N, 3.7. **Complex 3.3 a·H_2O**: ^{1}H-NMR (400 MHz, CD_2Cl_2, 25 °C): δ = 7.73 (br, 8H, H_{ortho}-BAr^F), 7.57 (br, 4H, H_{para}-BAr^F), 6.96–6.88 (m, 6 H, CH-Mes), 6.83 and 6.78 (s, 1H each, CH-Mes), 2.45, 2.43, 2.41 and 2.38 (s, 12H global, CH_3), 2.05 (d, 1H, $J_{H,H}$ = 16.5 Hz, CH_2-Bpin), 1.83–1.61 (s, 33H global, CH_3), 1.49 (d, 1H, $J_{H,H}$ = 16.5, CH_2-Bpin), 1.15 (s, 12H, CH_3-Bpin), −28.3 (s + d, 1H, $J_{Pt,H}$ = 1907.4 Hz, Pt–H). ^{13}C{^{1}H} NMR (100 MHz, CD_2Cl_2, 25 °C): δ = 173.9 and 173.4 (Pt=C), 162.2 (q, $J_{C,B}$ = 50 Hz, C_{ipso}-BAr^F), 139.3, 139.2, 139.0, 138.8, 137.2, 136.22. 136.16, 135.8, 135.47, 135.44, 134.5 and 133.6 (C_q, Mes), 135.2 (br, C_{ortho}-BAr^F), 129.7, 129.6, 129.5, 129.3 and 128.1 (br, CH-Mes), 129.3 (br q, $J_{C,F}$ = 30 Hz, C_{meta}-BAr^F), 125.8, 125.7, 125.6 and 125.5 (=C–CH_3), 125.1 (q, $J_{C,F}$ = 272 Hz, CF_3-BAr^F), 117.9 (br, C_{para}-BAr^F), 85.0 (C_q-Bpin), 24.8 and 24.4 (CH_3-Bpin), 21.4, 21.3, 18.5, 17.8, 17.7 and 17.6 (CH_3-Mes), 14.6 (very broad, CH_2-Bpin), 9.4, 9.2 and 9.1 (1:1:2 ratio, =C–CH_3). ^{11}B{^{1}H}(128 MHz, CD_2Cl_2, 25 °C): δ = 32.5 (very broad, Bpin), −6.6 (s, BAr^F). Elemental analysis calcd (%) for $C_{85}H_{72}B_2F_{24}N_4O_3Pt$: C, 55.41; H, 4.44; N, 3.63; Found: C, 55.6; H, 4.6; N, 3.7. **Complex 3.3 a·py**: ^{1}H-NMR (400 MHz, CD_2Cl_2, 25 °C): δ = 7.74 (br, 8H, H_{ortho}-BAr^F), 7.58 (br, 4H, H_{para}-BAr^F), 7.52 (t, 1H, $J_{H,H}$ = 7.5 Hz, CH-py), 7.04 (d, 2H, $J_{H,H}$ = 7.6 Hz, CH-py), 6.91–6.78 (m, 10 H, CH-Mes and CH-py), 2.43 (br, 12H, CH_3-Mes), 1.74 (s, 3H, CH_3), 1.70 (d, 1H, $J_{H,H}$ = 16.1, CH_2-Bpin), 1.66 (br, 9H, CH_3), 1.57 (br, 3H, CH_3), 1.53 and 1.50 s, 3H each, CH_3), 1.38 (d, 1H, $J_{H,H}$ = 16.1, CH_2-Bpin), 1.16 and 1.13 (s, 6H each, CH_3-Bpin), −20.5 (s + d, 1H, $J_{Pt,H}$ = 1386.0 Hz, Pt–H). ^{13}C{^{1}H} NMR (100 MHz, CD_2Cl_2, 25 °C): δ = 170.4 and 170.3 (Pt=C), 162.2 (q, $J_{C,B}$ = 50 Hz, C_{ipso}-BAr^F), 151.6 (CH-py), 139.05, 139.01, 138.96, 138.7 and 137.7 (2:1:1:1:1 ratio, C_q, Mes), 136.6 (CH-py), 136.13, 136.08, 136.0 (2:2:2 ratio, C_q, Mes), 135.2 (br, C_{ortho}-BAr^F), 134.8, 134.7 and 134.3 (1:2:1 ratio, C_q, Mes), 129.43 (br, CH-Mes), 129.3 (br q, $J_{C,F}$ = 30 Hz, C_{meta}-BAr^F), 128.8 (CH-py), 125.5, 125.3 and 125.2 (=C–CH_3), 125.1 (q, $J_{C,F}$ = 272 Hz, CF_3-BAr^F), 117.9 (br, C_{para}-BAr^F), 83.8 (C_q-Bpin), 25.0 and 24.7 (CH_3-Bpin), 21.4, 21.3, 17.9, 17.8 and 17.7 (CH_3-Mes), 16.2 (br, CH_2-Bpin), 9.5 and 9.2 (=C–CH_3). ^{11}B{^{1}H}(128 MHz, CD_2Cl_2, 25 °C): δ = 32.7 (very broad, Bpin), −6.6 (s, BAr^F). Elemental analysis calcd (%) for $C_{89}H_{75}B_2F_{24}N_5O_2Pt$: C, 55.41; H, 4.44; N, 3.63; Found: C, 55.6; H, 4.6; N, 3.7.

Synthesis of complexes 4.2 a, b and 4.3 a, b. *General procedure*: Cyclometallated complexes **1.2** or **1.3** (0.048 mmol) were dissolved in 0.4 mL of CH_2Cl_2 (or CD_2Cl_2 for monitoring the reactions) and transferred to a J. Young NMR tube with a screw cap. Thereafter, H_2 was introduced at 3 bar to form in situ the corresponding platinum hydride derivatives [Pt(H)$(IMes)_2$][BAr^F], **5.2**, or [Pt(H)$(IMes^*)_2$][BAr^F], **5.3**.[26] After 30 min, this solution was transferred via cannula to a solution of the corresponding borane (0.144 mmol for HBpin or 0.072 mmol for HBcat) in 0.3 mL of CH_2Cl_2 (or CD_2Cl_2). The reactions with HBcat leading to complexes **4.2 b** and **4.3 b** take place at rt with full conversion after 30 min (gas evolution with a color change from colorless to yellow is observed). Reactions with HBpin to yield complexes **4.2 a** and **4.3 a** required heating at 60 °C over a period of 24 h. The solvent was then removed under vacuum and the yellow solids washed with pentane (3×4 mL). Although spectroscopic yields were high, the isolated yields decreased due to partial solubility of the final products in pentane. Crystals suitable for X-ray diffraction studies were grown from concentrated CH_2Cl_2 solution of the complexes into pentane or hexamethyldisiloxane. (Yields: **4.2 a**: 65%; **4.3 a**: 54%; **4.2 b**: 76%; **4.3 b**: 60%). **Complex 4.2 a**: ^{1}H-NMR (400 MHz, CD_2Cl_2, 25 °C): δ = 7.73 (br, 8H, H_{ortho}-BAr^F), 7.56 (br, 4H, H_{para}-BAr^F), 6.97 (br s, 4H, =CH), 6.91 (s, 8H, Mes), 2.42 (s, 12H, CH_3-Mes), 1.85 (s, 24H, CH_3-Mes), 0.76 (s, 12H, CH_3-Bpin). ^{13}C{^{1}H} NMR (100 MHz, CD_2Cl_2, 25 °C): δ = 186.7 (Pt=C), 162.2 (q, $J_{C,B}$ = 50 Hz, C_{ipso}-BAr^F), 139.7 (C_q, Mes), 135.4 (br, C_{ortho}-BAr^F), 135.1 (C_q-N), 129.8 (CH-Mes), 129.3 (br q, $J_{C,F}$ = 30 Hz, C_{meta}-BAr^F), 125.1 (q, $J_{C,F}$ = 272 Hz, CF_3-BAr^F), 123.7 (=CH), 117.9 (br, C_{para}-BAr^F), 84.6 (C_q-Bpin), 24.2 (CH_3-Bpin), 21.3 and 18.6 (1:2 ratio, CH_3-Mes). ^{11}B{^{1}H}(128 MHz, CD_2Cl_2, 25 °C): δ = −6.6 (s, BAr^F) (the signal for the Bpin fragment is too broad to be observable). Elemental analysis calcd (%) for $C_{80}H_{72}B_2F_{24}N_4O_2Pt$: C, 53.56; H, 4.04; N, 3.12; Found: C, 53.5; H, 3.9; N, 3.4. **Complex 4.3 a**: ^{1}H-NMR (400 MHz, CD_2Cl_2, 25 °C): δ = 7.73 (br, 8H, H_{ortho}-BAr^F), 7.57 (br, 4H, H_{para}-BAr^F), 6.88 (s, 8H, Mes), 2.43 (s, 12H, CH_3-Mes), 1.78 (s. 24H, CH_3-Mes), 1.71 (=C–CH_3), 0.85 (s, 12H, CH_3-Bpin). ^{13}C{^{1}H} NMR (100 MHz, CD_2Cl_2, 25 °C): δ = 184.4 (Pt=C), 162.2 (q, $J_{C,B}$ = 50 Hz, C_{ipso}-BAr^F), 139.2 (C_q, Mes), 135.5 (C_q-Mes), 135.2 (br, C_{ortho}-BAr^F), 134.0 (C_q-N), 129.7 (CH-Mes), 129.1 (br q, $J_{C,F}$ = 30 Hz, C_{meta}-BAr^F), 127.0 (=C–*CH_3*), 125.0 (q, $J_{C,F}$ = 272 Hz, CF_3-BAr^F), 117.9 (br, C_{para}-BAr^F), 84.3 (C_q-Bpin), 24.4 (CH_3-Bpin), 21.4 and 18.5 (1:2 ratio, CH_3-Mes), 9.2 (=C–CH_3). ^{11}B{^{1}H}(128 MHz, CD_2Cl_2, 25 °C): δ = 4.5 (very broad, Bpin), −6.6 (s, BAr^F). Elemental analysis calcd (%) for $C_{84}H_{80}B_2F_{24}N_4O_2Pt$: C, 54.53; H, 4.36; N, 3.03; Found: C, 54.4; H, 4.2; N, 3.1. **Complex 4.2 b**: ^{1}H-NMR (400 MHz, CD_2Cl_2, 25 °C): δ = 7.75 (br, 8H, H_{ortho}-BAr^F), 7.58 (br, 4H, H_{para}-BAr^F), 7.00 (br s, 4H, =CH), 6.90 (m, 2H, Bcat), 6.78 (s, 8H, CH-Mes), 6.70 (m, 2H, Bcat), 2.25 (s, 12H, CH_3-Mes), 1.82 (s, 24H, CH_3-Mes). ^{13}C{^{1}H} NMR (100 MHz, CD_2Cl_2, 25 °C): δ = 183.4 (Pt=C), 162.2 (q, $J_{C,B}$ = 50 Hz, C_{ipso}-BAr^F), 149.0 (C_q-Bcat), 140.5 (C_q, Mes), 135.2 (br, C_{ortho}-BAr^F), 133.7 (C_q-N), 129.8 (CH-Mes), 129.3 (br q, $J_{C,F}$ = 30 Hz, C_{meta}-BAr^F), 125.1 (q, $J_{C,F}$ = 272 Hz, CF_3-BAr^F), 123.5 (=CH), 121.9 (CH-Bcat), 117.9 (br, C_{para}-BAr^F), 111.4 (CH-Bcat), 21.2 and 18.0 (1:2 ratio, CH_3-Mes). ^{11}B{^{1}H}(160 MHz, CD_2Cl_2, 25 °C): δ = 5.9 (s + d, very broad, Bcat, $J_{Pt,B}$ ~1700 Hz), −6.6 (s, BAr^F). Elemental analysis calcd (%) for $C_{80}H_{60}B_2F_{24}N_4O_2Pt$: C, 53.80; H, 3.61; N, 3.14; Found: C, 53.5; H, 4.1; N, 3.1. **Complex 4.3 b**: ^{1}H-NMR (400 MHz, CD_2Cl_2, 25 °C): δ = 7.74 (br, 8H, H_{ortho}-BAr^F), 7.57 (br, 4H, H_{para}-BAr^F), 6.90 (m, 2H, CH-Bcat), 6.79 (s, 8H, Mes), 6.72 (m, 2H, CH-Bcat) 2.27 (s, 12H, CH_3-Mes), 1.75 (s, 12H, =C–CH_3), 1.70 (s. 24H, CH_3-Mes). ^{13}C{^{1}H} NMR (100 MHz, CD_2Cl_2, 25 °C): δ = 181.1 (Pt=C), 162.2 (q, $J_{C,B}$ = 50 Hz, C_{ipso}-BAr^F), 149.1 (C_q-Bcat), 140.2 (C_q-Mes), 135.7 (C_q, Mes), 135.2 (br, C_{ortho}-BAr^F), 132.4 (C_q-N), 129.7 (CH-Mes), 129.1 (br q, $J_{C,F}$ = 30 Hz, C_{meta}-BAr^F), 127.0 (=C–CH_3), 125.0 (q, $J_{C,F}$ = 272 Hz, CF_3-BAr^F), 121.8 (CH-Bcat), 117.9 (br, C_{para}-BAr^F), 111.4 (CH-Bcat), 21.2 and 17.8 (1:2 ratio, CH_3-Mes), 9.0 (=C–CH_3). ^{11}B{^{1}H}(128 MHz, CD_2Cl_2, 25 °C): δ = 6.2 (very broad, Bcat, $J_{Pt,B}$ ~1700 Hz)), −6.6 (s, BAr^F). Elemental analysis calcd (%) for $C_{84}H_{72}B_2F_{24}N_4O_2Pt$: C, 54.77; H, 3.94; N, 3.04; Found: C, 53.5; H, 4.1; N, 3.1.

Synthesis of complex 4.3 e. Cyclometallated complex **1.3** (80 mg, 0.046 mmol) was dissolved in 0.7 mL of CH_2Cl_2 (or CD_2Cl_2 for monitoring the reactions) and $HBMe_2Bdab$ (20 mg, 0.14 mmol) was added. The solution stirred for 40 h a rt until all **1.3** complex was consumed. The solvent was removed under vacuum and the light yellow residue washed with pentane to remove the excess $HBMe_2Bdab$. Attempts to purify this complex by crystallization were unsuccessful and side products remained together with complex **4.3 e. Complex 4.3 e**: ^{1}H-NMR (400 MHz, CD_2Cl_2, 25 °C): δ = 7.73 (br, 8H, H_{ortho}-BAr^F), 7.57 (br, 4H, H_{para}-BAr^F), 6.82 (s, 8H, Mes), 6.81 (m, 2H, CH-Bdab), 6.49 (m, 2H, CH-Bdab) 2.33 (s, 6 H, N–CH_3), 2.31 (s, 12H, CH_3-Mes), 1.66 (s, 12 H, =C–CH_3), 1.63 (s, 24H, CH_3-Mes). ^{13}C{^{1}H}

NMR (100 MHz, CD_2Cl_2, 25 °C): δ = 180.1 (Pt=C), 162.2 (q, $J_{C,B}$ = 50 Hz, C_{ipso}-BAr^F), 139.9 (C_q-Bdab), 140.2 (C_q-Mes), 135.6 (C_q, Mes), 135.2 (br, C_{ortho}-BAr^F), 133.1 (C_q-N), 129.8 (CH-Mes), 129.1 (br q, $J_{C,F}$ = 30 Hz, C_{meta}-BAr^F), 127.3 (=C–CH_3), 125.0 (q, $J_{C,F}$ = 272 Hz, CF_3-BAr^F), 117.8 (CH-Bdab), 117.9 (br, C_{para}-BAr^F), 106.5 (CH-Bdab), 31.4 (N–CH_3), 21.2 and 18.1 (1 : 2 ratio, CH_3-Mes), 9.1 (=C–CH_3). $^{11}B\{^1H\}$(128 MHz, CD_2Cl_2, 25 °C): δ = 10.1 (very broad, Bcat, $J_{Pt,B}$ ~ 1300 Hz)), −6.6 (s, BAr^F).

The x-ray crystallographic coordinates for structures **2.1 d**, **2.1 e**, **3.2 a·H_2O**, **4.1 e**, **4.2 a** and **4.3 b** have been deposited under deposition numbers 2083230–2083235.

Deposition Numbers 2083230 (for **4.1e**), 2083231 (for **4.2a**), 2083232 (for **4.3b**), 2083233 (for **3.2a**), 2083234 (for **2.1e**), and 2083235 (for **2.1d**) contain the supplementary crystallographic data for this paper. These data are provided free of charge by the joint Cambridge Crystallographic Data Centre and Fachinformationszentrum Karlsruhe Access Structures service www.ccdc.cam.ac.uk/structures.

Acknowledgements

Financial support (FEDER contribution) from the Ministerio de Ciencia e Innovación (Projects PID-2020-116861GB-I00, PID2019-109312GB-I00 and RED2018-102387-T), the CSIC (AEPP_CTQ2016-76267-P) and the use of computational facilities of the Supercomputing Center of Galicia (CESGA) is gratefully acknowledged.

Conflict of Interest

The authors declare no conflict of interest.

Keywords: Borane · Boron · Density-functional calculations · Platinum · Structure elucidation

[1] a) L. J. Donnelly, S. Parsons, C. A. Morrison, S. P. Thomas, J. B. Love, *Chem. Sci.* **2020**, *11*, 9994–9999; b) M. A. Esteruelas, A. Martínez, M. Oliván, E. Oñate, *Chem. Eur. J.* **2020**, *26*, 12632–12644; c) B. J. Foley, N. Bhuvanesh, J. Zhou, O. Ozerov, *ACS Catal.* **2020**, *10*, 9824–9836; d) H. Shao, Y. Wang, C. W. Bielawski, P. Liub, *ACS Catal.* **2020**, *10*, 3820–3827; e) J. C. Babón, M. A. Esteruelas, I. Fernández, A. M. López, E. Oñate, *Organometallics* **2020**, *39*, 3864–3872; f) B. Ghaffari, B. A. Vanchura, G. A. Chotana, R. J. Staples, D. Holmes, R. E. Maleczka, M. R. Smith, *Organometallics* **2015**, *34*, 4732–4740; g) C. J. Wallis, G. Alcaraz, A. S. Petit, A. I. Poblador-Bahamonde, E. Clot, C. Bijani, L. Vendier, S. Sabo-Etienne, *Chem. Eur. J.* **2015**, *21*, 13080–13090; h) C. M. Kelly, J. T. Fuller III, C. M. Macaulay, R. McDonald, M. J. Ferguson, S. M. Bischof, O. L. Sydora, D. H. Ess, M. Stradiotto, L. Turculet, *Angew. Chem. Int. Ed.* **2017**, *56*, 6312–6316; *Angew. Chem.* **2017**, *129*, 6409–6413; i) H. Braunschweig, P. Brenner, R. D. Dewhurst, F. Guethlein, J. O. C. Jimenez-Halla, K. Radacki, J. Wolf, L. Zöllner, *Chem. Eur. J.* **2012**, *18*, 8605–8609; j) I. A. I. Mkhalid, J. H. Barnard, T. B. Marder, J. M. Murphy, J. F. Hartwig, *Chem. Rev.* **2010**, *110*, 890–931; k) K. K. Pandey, *Coord. Chem. Rev.* **2009**, *253*, 37–55; l) W. H. Lam, K. C. Lam, Z. Lin, S. Shimada, R. N. Perutz, T. B. Marder, *Dalton Trans.* **2004**,1556–1562

[2] a) M. A. Esteruelas, A. M. López, M. Oliván, *Chem. Rev.* **2016**, *116*, 8770–8847; b) I. M. Riddlestone, J. A. B. Abdalla, S. Aldridge, *Adv. Organomet. Chem.* **2015**, *63*, 1–38; c) G. Alcaraz, M. Grellier, S. Sabo-Etienne, *Acc. Chem. Res.* **2009**, *42*, 1640–1649; d) Z. Lin, *Transition Metal σ-borane complexes, in Contemporary metal boron chemistry I: borylenes, boryls, borane σ-complexes and borohydrides*, (Eds.: T. B. Marder, Z. Lin) Springer, **2008**, *vol. 130*, pp. 123–148; For some recent examples of agostic BH complexes see: e) J. J. Race, A. L. Burnage, T. M. Boyd, A. Heyam, A. J. Martínez-Martínez, S. A. Macgregor, A. S. Weller, *Chem. Sci.* **2021**, *12*, 8832–8843; f) M. W. Drover, L. L. Schafer, J. A. Love, *Angew. Chem. Int. Ed.* **2016**, *55*, 3181–3186; *Angew. Chem.* **2016**, *128*, 3233–3238; g) W.-C. Shih, W. Gu, M. C. MacInnis, S. D. Timpa, N. Bhuvanesh, J. Zhou, O. V. Ozerov, *J. Am. Chem. Soc.* **2016**, *138*, 2086–2089; h) A. F. Hill, C. M. A. McQueen, *Organometallics* **2014**, *33*, 1977–1985; i) M. Hasegawa, Y. Segawa, M. Yamashita, K. Nozaki, *Angew. Chem. Int. Ed.* **2012**, *51*, 6956–6960; *Angew. Chem.* **2012**, *124*, 7062–7066; j) Y. Gloaguen, G. Alcaraz, A. S. Petit, E. Clot, Y. Coppel, L. Vendier, S. Sabo-Etienne, *J. Am. Chem. Soc.* **2011**, *133*, 17232–17238; k) Y. Gloaguen, G. Alcaraz, A.-F. Pécharman, E. Clot, L. Vendier, S. Sabo-Etienne, *Angew. Chem. Int. Ed.* **2009**, *48*, 2964–2968; *Angew. Chem.* **2009**, *121*, 3008–3012.

[3] a) M. T. Whited, B. L. H. Taylor, *Comments Inorg. Chem.* **2020**, *40*, 217–276; b) J. Y. Corey, *Chem. Rev.* **2016**, *116*, 11291–11435; c) R. H. Crabtree, *Chem. Rev.* **2016**, *116*, 8750–8769; d) G. J. Kubas, *Chem. Rev.* **2007**, *107*, 4152–4205; e) G. J. Kubas, *Proc. Natl. Acad. Sci. USA* **2007**, *104*, 6901–6907; f) G. I. Nikonov, *Adv. Organomet. Chem.* **2005**, *53*, 217–309.

[4] G. Alcaraz, S. Sabo-Etienne, *Coord. Chem. Rev.* **2008**, *252*, 2395–2409.

[5] a) A. Caballero, S. Sabo-Etienne, *Organometallics* **2007**, *26*, 1191–1195; b) C. Gunanathan, M. Hölscher, F. Pan, W. Leitner, *J. Am. Chem. Soc.* **2012**, *134*, 14349.14352 ; c) V. Montiel-Palma, M. Lumbierres, B. Donnadieu, S. Sabo-Etienne, B. Chaudret, *J. Am. Chem. Soc.* **2002**, *124*, 5624–5625; d) D. R. Lantero, S. L. Miller, J.-Y. Cho, D. L. Ward, M. R. Smith III, *Organometallics* **1999**, *18*, 235–247; e) H. Wadepohl, *Angew. Chem. Int. Ed.* **1997**, *36*, 2441–2444; *Angew. Chem.* **1997**, *109*, 2547–2550.

[6] J. F. Hartwig, *Chem. Soc. Rev.* **2011**, *40*, 1992–2002.

[7] Y. Wang, J. Bai, Y. Yang, W. Zhao, Y. Liang, D. Wang, Y. Zhao, Z. Shi, *Chem. Sci.* **2021**, *12*, 3599–3607.

[8] R. N. Perutz, S. Sabo-Etienne, *Angew. Chem. Int. Ed.* **2007**, *46*, 2578–2592; *Angew. Chem.* **2007**, *119*, 2630–2645.

[9] a) A. Cassen, Y. Gloaguen, L. Vendier, C. Duhayon, A. Poblador-Bahamonde, C. Raynaud, E. Clot, G. Alcaraz, S. Sabo-Etienne, *Angew. Chem. Int. Ed.* **2014**, *53*, 7569–7573; *Angew. Chem.* **2014**, *126*, 7699–7703; b) C. Y. Tang, A. L. Thompson, S. Aldridge, *J. Am. Chem. Soc.* **2010**, *132*, 10578–10591.

[10] P. Ríos, R. Martín-de la Calle, P. Vidossich, F. J. Fernández-de-Córdova, A. Lledós, S. Conejero, *Chem. Sci.* **2021**, *1*, 1647–1655.

[11] P. Ríos, H. Fouilloux, P. Vidossich, J. Díez, A. Lledós, S. Conejero, *Angew. Chem. Int. Ed.* **2018**, *57*, 3217–3221; *Angew. Chem.* **2018**, *130*, 3271–3275.

[12] a) H. Braunschweig, P. Brenner, R. D. Dewhurst, F. Guethlein, J. O. C. Jimenez-Halla, K. Radacki, J. Wolf, L. Zöllner, *Chem. Eur. J.* **2012**, *18*, 8605–8609; b) N. Arnold, H. Braunschweig, P. Brenner, J. O. C. Jimenez-Halla, T. Kupfer, K. Radacki, *Organometallics* **2012**, *31*, 1897–1907; c) H. Braunschweig, R. Bertermann, P. Brenner, M. Burzler, R. D. Dewhurst, K. Radacki, F. Seeler, *Chem. Eur. J.* **2011**, *17*, 11828–11837; d) H. Braunschweig, K. Radacki, K. Uttinger, *Chem. Eur. J.* **2008**, *14*, 7858–7866; e) H. Braunschweig, K. Radacki, D. Rais, D. Scheschkewitz, *Angew. Chem. Int. Ed.* **2005**, *44*, 5651–5654; *Angew. Chem.* **2005**, *117*, 5796–5799; f) G. J. Irvine, M. J. G. Lesley, T. B. Marder, N. C. Norman, C. R. Rice, E. G. Robins, W. R. Roper, G. R. Whittell, L. J. Wright, *Chem. Rev.* **1998**, *98*, 2685–2722.

[13] a) J. C. Babón, M. A. Esteruelas, I. Fernández, A. M. López, E. Oñate, *Inorg. Chem.* **2018**, *57*, 4482–4491; b) M. A. Esteruelas, I. Fernández, C. García-Yebra, J. Martín, E. Oñate, *Organometallics* **2017**, *36*, 2298–2307; c) K. K. Pandey, *Inorg. Chem. Commun.* **2008**, *11*, 288–292.

[14] Half-arrow notation has been used in the representation of the σ-BH complexes to distinguish between η^1 and η^2 coordination modes following the recommendations by Parkin and Green in: J. C. Green, M. L. H. Green, G. Parkin, *Chem. Commun.* **2012**, *48*, 11481–11503.

[15] The ^{11}B NMR chemical shifts for these cationic systems are considerably upfield-shifted in comparison with related neutral platinum systems bearing BMe_2dab. See: a) C. Borner, C. Kleeber, *Eur. J. Inorg. Chem.* **2014**, 2486–2489; b) H. Ogawa, M. Yamashita, *Dalton Trans.* **2013**, *42*, 625–629.

[16] The closest carbon atom to the vacant site is at 3.0 Å indicating that agostic interactions, if present, are weak.

[17] O. Rivada-Wheelaghan, M. A. Ortuño, J. Díez, A. Lledós, S. Conejero, *Angew. Chem. Int. Ed.* **2012**, *51*, 3936–3939; *Angew. Chem.* **2012**, *124*, 4002–4005.

[18] P. Ríos, H. Fouilloux, J. Díez, P. Vidossich, A. Lledós, S. Conejero, *Chem. Eur. J.* **2019**, *25*, 11346–11355.

[19] For a related carbon–boron bond coupling process with an iridium complex bearing an IMes ligand see: J. Navarro, O. Torres, M. Martín, E. Sola, *J. Am. Chem. Soc.* **2011**, *133*, 9738–9740.

[20] Attempts to purify these complexes by washing with pentane or by crystallization resulted in the inevitable change of the nature of the complexes according to their NMR spectra that based on several experiments carried out in the presence of added water correspond to formation of water adducts.
[21] J. Zhu, Z. Lin, T. B. Marder, *Inorg. Chem.* **2005**, *44*, 9384–9390.
[22] Even though the difference in Gibbs Energy between **3.2a** and **3.2a·H_2O** falls within the error of DFT methods (see M. Bogojeski, L. Vogt-Maranto, M. E. Tuckerman, K.-R. Muller, K. Burke, *Nat. Commun.* **2020**, *11*, 5223–5233), using BS1 (see supplementary information) gives the following values: $-3.3\ kcal\,mol^{-1}$ for **3.2a** and $-6.7\ kcal\,mol^{-1}$ for **3.2a·H_2O**, which matches the experimental observations.
[23] M. A. Ortuño, P. Vidossich, S. Conejero, A. Lledós, *Angew. Chem. Int. Ed.* **2014**, *53*, 14158–14161.
[24] We have observed previously some important differences between IMes and IMes* platinum complexes in the activation of C–H bonds of aromatic compounds. See Ref. [17] for details.
[25] S. W. Hadebe, R. S. Robinson, *Eur. J. Org. Chem.* **2006**, *4898*.
[26] O. Rivada-Wheelaghan, M. Roselló-Merino, M. A. Ortuño, P. Vidossich, E. Gutiérrez-Puebla, A. Lledós, S. Conejero, *Inorg. Chem.* **2014**, *53*, 4257–4268.

Manuscript received: May 19, 2021
Revised manuscript received: June 18, 2021
Accepted manuscript online: June 21, 2021